

## In Situ Fabrication of A Water-Soluble, Self-Doped Polyaniline Nanocomposite: The Unique Role of DNA Functionalized Single-Walled Carbon Nanotubes

Yufeng Ma, Shah R. Ali, Ling Wang, Pui Lam Chiu, Richard Mendelsohn, and Huixin He\*

Department of Chemistry, Rutgers University, 73 Warren Street, Newark, New Jersey 07102

Received May 24, 2006; E-mail: huixinhe@newark.rutgers.edu

Tremendous efforts have been made over the past decade to prepare polymer and carbon nanotube (CNT) composites with an aim to synergistically combine the merits of each individual component.<sup>1</sup> In situ polymerization of the respective monomers in the presence of carbon nanotubes is expected to form a genuine polymer/CNT composite with much more enhanced functions compared to the “post mixing” approaches.<sup>1e–f</sup> However, in situ polymerization requires predispersing the carbon nanotubes into solution. Different dispersion approaches have been reported, such as polymer wrapping,<sup>2</sup> noncovalent adhesion of molecules,<sup>3</sup> and acidic oxidation,<sup>4</sup> which impart different surface chemistries and electronic structures to the carbon nanotubes. The expected improvement in the nanocomposites is critically dependent on the polymer-nanotube interfacial chemical and electronic interactions. Recent interest has been directed at the effect of the interfacial interaction<sup>5</sup> on the mechanical and electronic enhancement in the composites. However, the impact of dispersion and functionalization of the carbon nanotubes on the molecular structure of the polymer in a composite, and therefore on the chemical stability and the performance of the composite, has not yet been addressed.

Here we report that dispersion and functionalization of single-walled carbon nanotubes (SWNTs) with single-stranded DNA (ss-DNA, dT30)<sup>2,6</sup> can dramatically change the molecular structure and performance of the polymer in the nanocomposite. In this communication, a water-soluble self-doped polyaniline/SWNT nanocomposite was produced by in situ polymerization of 3-aminophenylboronic acid monomers in the presence of DNA functionalized SWNTs.<sup>6</sup> The polyaniline (PANI) backbone in the produced poly-(anilineboronic acid)/ss-DNA/SWNT (PABA/ss-DNA/SWNT) composite had longer conjugated structures and was more in the stable emeraldine state than in the degradable pernigraniline state, which can greatly enhance the chemical stability of the self-doped PANI. The fact that ss-DNA functionalized SWNTs did not promote quinoid unit formation in the PANI backbone is the *reverse* of previous reports on PANI/CNT composites.<sup>1d–f</sup> In addition, the conductance of the composite is  $385 \pm 6$  and  $245 \pm 20$  times higher than the simple sum of the conductance of pure PABA and ss-DNA/SWNTs alone in the doped and dedoped states, respectively.

UV–vis absorption spectra have been widely used to determine the oxidation states of PANI because of their distinct chromatic properties.<sup>7</sup> Figure 1a shows the UV–vis spectra of the composite solution (—) and the pure PABA solution (—, inset), which were polymerized at 0 °C for 12 h.<sup>6</sup> Two broad peaks appear with maxima at 365 and 628 nm for the pure PABA solution, which are assigned to  $\pi$ – $\pi^*$  and aromatic–quinoid transitions, respectively.<sup>7</sup> For the composite, the peaks appear at 420 and 900 nm. These two peaks have been assigned to polaron and delocalized bipolaron structures in the conductive, partially oxidized emeraldine salt state.<sup>7</sup> These results lead to a conclusion that the PABA in the composite is in the more conductive and stable emeraldine state, while the

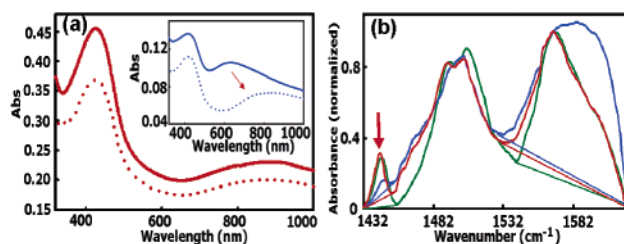


**Figure 1.** (a) UV–vis spectra of the PABA/ss-DNA/SWNT composite (red) and the pure PABA (inset, blue) before (—) and after (···) treatment with NaBH<sub>4</sub>; (b) FTIR spectra of the composite (red) and the pure PABA (blue) and the pure PABA after reduction with NaBH<sub>4</sub> (green). The spectra were normalized with the 1570 cm<sup>-1</sup> peak. Baselines for the absorption height ratio measurements are shown.

pure PABA exists more in the degradable, fully oxidized pernigraniline state.

To further support this conclusion, we reduced the as-synthesized pure PABA and composite with NaBH<sub>4</sub>.<sup>6</sup> Figure 1 shows the UV–vis absorption spectra of the materials after NaBH<sub>4</sub> reduction with dashed lines. The peak at 628 nm (Figure 1a inset, solid) greatly shifts to 811 nm (Figure 1a inset, dashed) for the pure polymer, revealing that most of the PABA in the as-synthesized pure polymer was in the oxidized PA state. However, for the composite, the peak at 900 nm barely shifted its position (Figure 1a), further demonstrating that the PABA existed more in the EB state in the composite. After reduction, the pure PABA still absorbs at a shorter wavelength (89 nm shorter) than the composite. This large difference may be due to strong electronic interactions between carbon nanotubes and the PABA. It is also possible that the polyaniline backbone has longer conjugated structures in the composite.

To understand the molecular structures of the PANI backbone in the pure PABA and in the composite, we used FTIR to examine the films prepared from the respective solutions.<sup>6</sup> Figure 1b shows the FTIR spectra of the pure PABA before (blue) and after reduction with NaBH<sub>4</sub> (green) and of the composite (red). All the spectra clearly exhibit benzenoid and quinoid ring vibrations at 1444 and 1570 cm<sup>-1</sup>, respectively. The ratio of the absorption heights of quinoid to benzenoid ring modes ( $I_{1570}/I_{1444}$ ) in the pure PABA is  $12 \pm 2$ , which suggests that the percentage of quinoid units is much higher than that of benzenoid units for the pure PABA film. This result is consistent with previous reports.<sup>7e,8</sup> However, the ratio of  $I_{1570}$  to  $I_{1444}$  decreases to  $2.7 \pm 0.3$  for the PABA in the composite, indicating that the relative amount of quinoid units decreased in the PABA when polymerized in the presence of the ss-DNA/SWNTs. Furthermore, reduction of the pure PABA with NaBH<sub>4</sub> results in a large decrease of the  $I_{1570}/I_{1444}$  ratio to  $2.0 \pm 0.1$ , similar to the ratio for the composite.<sup>9</sup> All these results further demonstrate that the PABA exists more in the fully oxidized pernigraniline state in pure PABA and more in the emeraldine state in the composite.

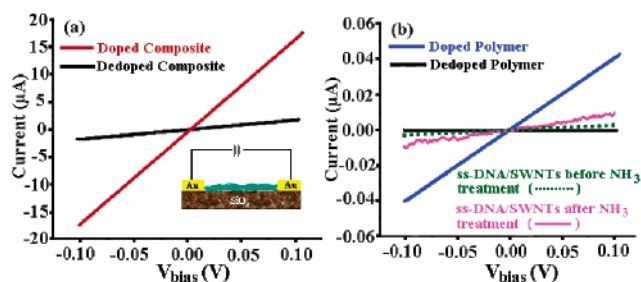


**Figure 2.** Typical  $I$ – $V$  characteristic curves of the (a) PABA-ss-DNA/SWNTs composite film, (b) PABA alone, and ss-DNA/SWNT alone before and after treatment with  $\text{NH}_3$ .

Aromatic molecules are known to interact strongly with the basal planes of graphitic surfaces via  $\pi$ – $\pi$  stacking. It has been demonstrated that a site-selective interaction between the quinoid ring of PANI and the nanotubes occurred as a consequence of the in situ polymerization. This interaction promotes and/or stabilizes the quinoid ring structures.<sup>1d–f</sup> Therefore we expected that the PABA in a composite should have more quinoid units than pure PABA. Our unexpected results may be due to the unique electronic properties of the DNA functionalized carbon nanotubes. Because of the electron donating ability of the DNA molecules, the ss-DNA/SWNTs become very different from bare carbon nanotubes<sup>10</sup> and nanotubes dispersed by strong acid oxidation,<sup>1d</sup> such that they are effective electron donors, and therefore possess reductive capability.<sup>11</sup> The reduction potential of pernigraniline is 1.04 V versus NHE.<sup>9</sup> The reduction potential of ss-DNA/SWNTs is 0.8 V versus NHE.<sup>11a</sup> Therefore the pernigraniline produced during the polymerization was readily reduced to the emeraldine state by the ss-DNA/SWNTs.

It is well-known that pernigraniline is not stable in aqueous solutions. PABA polymerized in situ with ss-DNA/SWNTs existing in the more stable emeraldine state suggests that the ss-DNA/SWNTs would greatly enhance the chemical stability of the film. In our earlier study,<sup>9</sup> we indeed found that the PABA had much more enhanced electrochemical stability when it was in situ electrochemically polymerized in the presence of ss-DNA/SWNTs compared to the pure PABA film. Therefore we draw the conclusion that the functionalization of SWNTs with DNA improved the quality and stability of the composite.

As expected, the electronic conductivity of the nanocomposite is greatly improved over the pure PABA. Figure 2 shows the current–voltage ( $I$ – $V$ ) curves measured on the films prepared from the composite and pure PABA solution. They all showed ohmic behavior between  $-0.1$  and  $0.1$  V. In the doped state, the conductance of the nanocomposite ( $\sim 1.8 \times 10^{-4}$  S) is  $\sim 390$  times higher than the pure PABA film ( $\sim 4.4 \times 10^{-7}$  S) even though these films are fabricated under the same conditions. After dedoping with ammonia<sup>6</sup> the conductance of the pure PABA is below  $10^{-11}$  S, which is beyond our instrumental measurement sensitivity. The nanocomposite is still conductive after dedoping, and the conductance decreased 7-fold to  $\sim 2.5 \times 10^{-5}$  S. This value is still  $\sim 54$  times higher than the conductance of pure PABA films in the doped state. Control experiments were performed with ss-DNA/SWNTs on the conductance measurements (Figure 2b). We found that the

conductance of the composite in the doped is  $385 \pm 6$  higher than the sum of the conductance of pure PABA and ss-DNA/SWNTs alone. In the dedoped state the conductance is  $245 \pm 20$  times higher. The mechanism for the enhanced conductivity needs further study. It may be because the PABA has a longer conjugated backbone and exists predominantly in the conductive emeraldine state in the composite. It is also possible that a strong electronic interaction between the PABA and the ss-DNA/SWNTs in the composite causes the synergistic enhancement of the conductance.<sup>12</sup> Other possible explanations are that the ss-DNA/SWNTs act as conductive polyanionic doping agents,<sup>1d</sup> or that the ss-DNA/SWNTs serve as “conducting bridges”, connecting PABA conducting domains and increasing the effective percolation.

In summary, we demonstrated that functionalization of carbon nanotubes dramatically impacts the molecular structure of the polymer in an in situ fabricated composite. We envision that rational design of the functionality of the carbon nanotubes can produce advanced nanocomposite materials with greatly improved performances.

**Acknowledgment.** Acknowledgment is made to the donors of the American Chemical Society Petroleum Research Fund for support of this research. We thank Ms. Xiulan Li and Prof. Nongjian Tao for their generous gift of Si chips for the conductivity measurements.

**Supporting Information Available:** Detailed explanation of experimental procedures. This material is available free of charge via the Internet at <http://pubs.acs.org>.

## References

- (1) (a) Iijima, S. *Nature* **1991**, *354*, 56. (b) Ajayan, P. M.; Stephan, O.; Colliex, C.; Trauth, D. *Science* **1994**, *265*, 1212. (c) Dai, L.; Mau, A. W. H. *Adv. Mater.* **2001**, *13*, 899–913. (d) Zengin, H.; Zhou, W.; Jin, J.; Czerw, R.; Smith, J. D. W.; Echegoyen, L.; Carroll, D. L.; Foulger, S. H.; Ballato, J. *Adv. Mater.* **2002**, *14*, 1480–1483. (e) Cochet, M.; Maser, W. K.; Benito, A. M.; Callejas, M. A.; Martínez, M. T.; Benoit, J.-M.; Schreiber, J.; Chauvet, O. *Chem. Comm.* **2001**, 1450. (f) Sainz, R.; Benito, A. M.; Martínez, M. T.; Galindo, J. F.; Sotres, J.; Baró, A. M.; Corraze, B.; Chauvet, O.; Maser, W. K. *Adv. Mater.* **2005**, *17*, 278–281.
- (2) Zheng, M.; Jagota, A.; Semke, E. D.; Diner, B. A.; Mclean, R. S.; Lustig, S. R.; Richardson, R. E.; Tassi, N. G. *Nat. Mater.* **2003**, *2*, 338–342.
- (3) (a) Chen, R. J.; Zhang, Y. G.; Wang, D. W.; Dai, H. J. *J. Am. Chem. Soc.* **2001**, *123*, 3838–3839. (b) Chen, J.; Liu, H. Y.; Weimer, W. A.; Halls, M. D.; Walkdeck, D. H.; Walker, G. C. *J. Am. Chem. Soc.* **2002**, *124*, 9034–9035.
- (4) Wang, Y.; Iqbal, Z.; Mitra, S. *J. Am. Chem. Soc.* **2006**, *128*, 95–99.
- (5) Chen, J.; Ramasubramaniam, R.; Xue, C.; Liu, H. *Adv. Funct. Mater.* **2006**, *16*, 114–119.
- (6) See Supporting Information.
- (7) (a) Stilwell, D. S.; Park, S.-M. *J. Electrochem. Soc.* **1989**, *136*, 427–433. (b) McManus, P. M.; Cushman, R. J.; Yang, S. C. *J. Phys. Chem. B* **1987**, *91*, 744–747. (c) de Albuquerque, J. E.; Mattoso, L. H. C.; Faria, R. M.; Masters, J. G.; MacDiarmid, A. G. *Synth. Met.* **2004**, *146*, 1–10. (d) Deore, B. A.; Hachey, S.; Freund, M. S. *Chem. Mater.* **2004**, *16*, 1426–1432. (e) Deore, B. A.; Yu, I.; Freund, M. S. *J. Am. Chem. Soc.* **2004**, *126*, 52–53.
- (8) Deore, B. A.; Yu, S.; Aguiar, P. M.; Recksiedler, C.; Kroeger, S.; Freund, M. S. *Chem. Mater.* **2005**, *17*, 3803–3805.
- (9) Ma, Y. F.; Ali, S. R.; Dodoo, A. S.; He, H. X. *J. Phys. Chem. B* **2006**, *110*, 16359–16365.
- (10) Shim, M.; Javey, A.; Kam, N. W. S.; Dai, H. J. *J. Am. Chem. Soc.* **2001**, *123*, 11512–11513.
- (11) (a) Zheng, M.; Diner, B. A. *J. Am. Chem. Soc.* **2004**, *126*, 15490. (b) Napier, M. E.; Hull, D. O.; Thorp, H. H. *J. Am. Chem. Soc.* **2005**, *127*, 11952–11953.
- (12) Zhao, B.; Hu, H.; Yu, A. P.; Perea, D.; Haddon, R. C. *J. Am. Chem. Soc.* **2005**, *127*, 8197–8203.

JA063375E